ACS OMEGA

http://pubs.acs.org/journal/acsodf

Article

A Potent Antioxidant Sesquiterpene, Abelsaginol, from *Abelmoschus sagittifolius*: Experimental and Theoretical Insights

Thuc Dinh Ngoc,* Mai Vu Thi Ha, Thanh Nguyen Le, Hue Vu Thi, Thi Van Anh Nguyen, Adam Mechler, Nguyen Thi Hoa, and Quan V. Vo*

Cite This: *ACS Omega* 2022, 7, 24004−24011

Read Online

ACCESS | Metrics & More | Article Recommendations | Supporting Information

ABSTRACT: The sesquiterpenoid compound abelsaginol (**AS**) was successfully isolated from *Abelmoschus sagittifolius* for the first time. The compound was identified using NMR and MS data. The antioxidant activity of **AS** was also evaluated both theoretically and experimentally. **AS** was found to be a weak HOO$^{\bullet}$ radical scavenger in organic solvents such as pentyl ethanoate and dimethyl sulfoxide ($k_{overall}$ = ∼ 10^2 M^{-1} s^{-1}), in a good agreement with the results of the 2,2′-azino-bis(3-ethylbenzothiazoline-6-sulfonic acid) assay. However, **AS** exhibited good HOO$^{\bullet}$ antiradical activity in water at pH 7.40 ($k_{overall}$ = 9.00 × 10^6 M^{-1} s^{-1}) through the single-electron transfer mechanism of the anion state. Further calculations also demonstrated that **AS** could exert good to moderate activity against $CH_3O^{\bullet}$, $CH_3OO^{\bullet}$, $CCl_3OO^{\bullet}$, NO_2, and $SO_4^{\bullet-}$ radicals, with k_f values from 4.00 × 10^3 to 1.52 × 10^7 M^{-1} s^{-1}. However, **AS** exerted much lower activity against HO$^{\bullet}$, $CCl_3O^{\bullet}$, NO, $O_2^{\bullet-}$, and $N_3^{\bullet}$ radicals under the studied conditions. In general, the activity of **AS** in water at pH 7.40 is higher than that of Trolox or butylated hydroxytoluene, which are common reference antioxidants. Thus, in an aqueous physiological milieu, **AS** is a promising natural antioxidant.

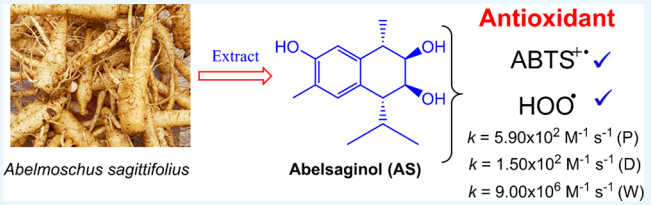

1. INTRODUCTION

Abelmoschus sagittifolius is a flowering plant that belongs to the *Abelmoschus* genus, which contains 15 species in the Malvaceae family. *Abelmoschus* was previously classified in the *Hibiscus* genus,[1] but the current botanic database classifies it as a distinct genus. The *A. sagittifolius* plant is distributed in Australia and Africa as well as tropical and subtropical Asian regions such as China, India, and Southeast Asian countries.[2,3] In Vietnamese and Chinese traditional medicine, the root tuber of *A. sagittifolius* is used for the treatment of cough, tuberculosis, constipation, neurasthenia, abscess, backache, headache, stomachache, phthisis, carbuncle sore, dizziness, and lumbosacral pain.[4−7] However, formal studies of the chemical composition and biological activity of *A. sagittifolius* have been limited. Chinese scientists have reported the isolation of sesquiterpenes, lignans, phenolic, and amide constituents from *A. sagittifolius*.[8−10] Several isolated compounds showed moderate cytotoxicities against HepG-2 and Hela cancer cell lines.[9,10] These limited data suggest that this traditional medicine does indeed contain potent natural products that can be isolated and tested for their activity. Recently, we isolated several known sesquiterpenes from the roots of *A. sagitifolis*.[11] Multiple chronic diseases are now know to be linked to oxidative stress.[12,13] The ability of natural products to scavenge free radicals is an important part of their antibacterial, anti-inflammatory, and cancer-prevention activities and it is the driving force behind antioxidant research.[14−17] In our continuing program of researching natural products, here we report the isolation and structural identification of a new sesquiterpenoid compound, abelsaginol (**AS**, Figure 1), that was tested for antioxidant activity both in vitro and in silico using quantum chemical calculations.

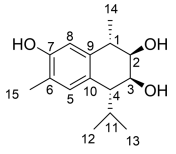

Abelsaginol (**AS**)

Figure 1. Molecular structure and atomic numbering of abelsaginol (**AS**).

2. RESULTS AND DISCUSSION

2.1. Isolation and Identification of AS from *A. sagittifolius*.

2.1.1. Isolation. The dried powder of the roots of *A. sagittifolius* (4.4 kg) was extracted with MeOH at room temperature for 24 h (20 L × 3 times). The extracts were

Received: May 12, 2022
Accepted: June 21, 2022
Published: July 1, 2022

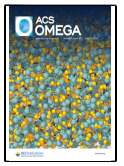

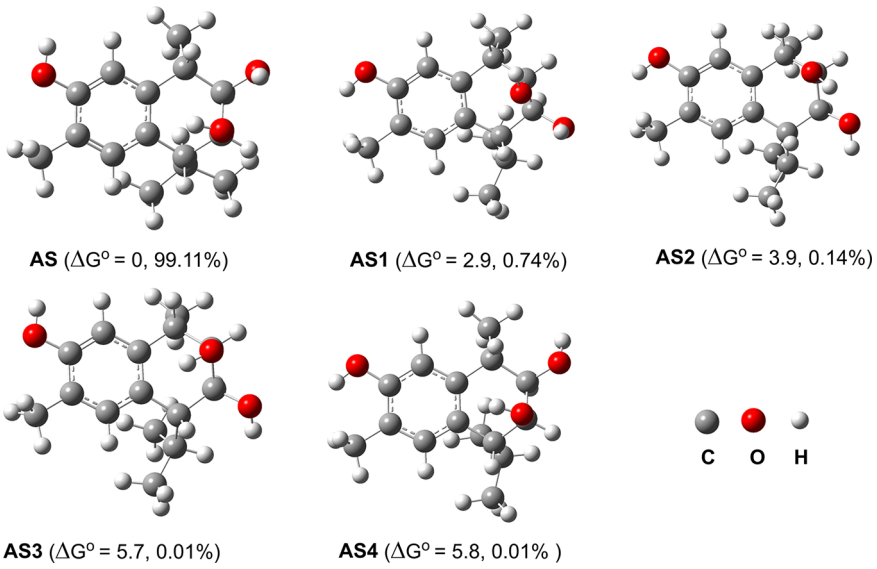

Figure 2. Typical conformers of **AS** and the relative free energies ΔG° (kcal mol^{-1}) compared to the **AS** conformer.

combined and concentrated under reduced pressure at 50 °C to obtain the MeOH residue. The MeOH residue was dissolved in 1 L of distilled water, and the mixture was extracted again with *n*-hexane and ethyl acetate, respectively. After distillation and the removal of the organic solvent, the *n*-hexane extract (46 g) and the ethyl acetate extract (7 g) were obtained.

The ethyl acetate residue (7 g) was subjected to silica gel column chromatography (CC), which was eluted with a gradient solvent system of *n*-hexane/ethyl acetate (from 0% to 100% ethyl acetate), and the fractions were confirmed by thin layer chromatography (TLC). Nine corresponding fractions were obtained (E1−E9).

The E4 fraction (64 mg) was purified by RP-18 reverse-phase silica gel column chromatography (YMC) with an enluent of MeOH/water (1/2) to obtain compound **1** (8.4 mg), a white amorphous powder. $[\alpha]_D^{25}$ −33.5 (*c* 0.2, MeOH). HR-ESI-MS *m*/*z*: 285.1253 $[M + Cl]^-$ ($C_{15}H_{22}O_3Cl$ calcd. 285.1257). ^1H NMR (500 MHz, $CDCl_3$) δ_H (ppm): 6.85 (1H, s, H-5), 6.60 (1H, s, H-8), 4.15 (1H, dd, *J* = 2.5 Hz, 4.0 Hz, H-3), 3.71 (1H, dd, *J* = 2.5, 7.0 Hz, H-2), 2.76 (1H, quin, *J* = 7.0 Hz, H-1), 2.61 (1H, dd, *J* = 4.0, 7.0 Hz, H-4), 2.18 (3H, s, H-15), 1.78 (1H, m, H-11), 1.38 (3H, d, *J* = 7.0 Hz, H-14), 0.99 (d, *J* = 7.0 Hz, H-13), 0.92 (d, *J* = 7.0 Hz, H-12). ^{13}C NMR (125 MHz, CD_3OD) δ_C (ppm): 152.7 (C-7), 137.9 (C-9), 132.8 (C-5), 127.2 (C-10), 121.8 (C-6), 113.9 (C-8), 73.7 (C-3), 70.4 (C-2), 51.7 (C-4), 38.2 (C-1), 32.7 (C-11), 21.9 (C-13), 20.2 (C-12), 19.7 (C-14), 15.5 (C-15).

2.1.2. Identification. Compound **1** was isolated from the ethyl acetate extract as a white amorphous powder with a molecular formula of $C_{15}H_{22}O_3$, as determined by HR-ESI-MS at *m*/*z* 285.1253 ($[M + Cl]^-$ $C_{15}H_{22}O_3Cl$ calcd. 285.1257), indicating five degrees of unsaturation. The ^1H NMR spectrum showed two aromatic proton signals at δ_H 6.85 (1H, s, H-5) and 6.60 (1H, s, H-8); two oxymethine groups at δ_H 4.15 (1H, dd, *J* = 2.5 Hz, 4.0 Hz, H-3) and 3.71 (1H, dd, *J* = 2.5, 7.0 Hz, H-2); three methine groups at δ_H 2.76 (1H, quin, *J* = 7.0 Hz, H-1), 2.61 (1H, dd, *J* = 4.0, 7.0 Hz, H-4), and 1.78 (1H, m, H-11); and four methyl groups at δ_H 2.18 (3H, s, H-15), 1.38 (3H, d, *J* = 7.0 Hz, H-14), 0.99 (d, *J* = 7.0 Hz, H-13), and 0.92 (d, *J* = 7.0 Hz, H-12). The ^{13}C NMR and HSQC spectra revealed 15 carbon signals, including six aromatic carbon signals at δ_C 152.7 (C-7), 137.9 (C-9), 132.8 (C-5), 127.2 (C-10), 121.8 (C-6), and 113.9 (C-8); two oxymethine carbons at δ_C 73.7 (C-3) and 70.4 (C-2); three methine group signals at δ_C 51.7 (C-4), 38.2 (C-1), and 32.7 (C-11); and four methyl signal at 21.9 (C-13), 20.2 (C −12), 19.7 (C-14), and 15.5 (C-15). The NMR spectral data suggested **1** was a cardinane-type sesquiterpene. The assignments of all hydrogen and carbon signals were done using $^1H-^1H$ COSY, HSQC, and HMBC correlations. The $^1H-^1H$ COSY correlations of the H-14/H-1/H-2/H-3/H-4/H-11/H-12 (and H-13) system were observed. The HMBC spectrum showed the correlations from H-5 (δ_H 6.85) to C-4 (δ_C 51.7), C-7 (δ_C 152.7), C-9 (δ_C 137.9), and H-15 (δ_C 15.5) and the correlations from H-8 (δ_H 6.60) to C-1 (δ_C 38.2), C-6 (δ_C1 21.8), and C-10 (δ_C 127.2) (Figure S1). Thus, the planar structure of **1** was suggested as 2,3,7-trihydroxycalamenene, similar to the aglycone of compound 2*β*,7,3*β*-trihydroxycalamenene 3-*O*-*β*-D-glucoside, which was isolated from the Chinese *A. sagittifolius* stem tuber by Chen et al.[8] The relative configurations of **1** were assigned using the NOESY spectrum and coupling constants. We found that compound **1** had the same relative configurations as 2*β*,7,3*β*-trihydroxycalamenene 3-*O*-*β*-D-glucoside at the C-1, C-2, and C-3 positions but a different relative configuration at the C-4 position. The NOESY correlation from H-2 (δ_H 3.71) to H-14 (δ_H 1.38) indicated that H-1 and H-2 were on opposite sides. The positions of H-1 and H-2 were further confirmed by the large coupling constant between H-1 and H-2 (*J* = 7.0 Hz). The small coupling constant between H-2 and H-3 (*J* = 2.5 Hz) suggested that H-2 and H-3 were on the same side. However, the isopropyl group at the C-4 position of **1** was assigned on the same side of the ring as H-2 and H-3 due to the NOESY correlations from H-2 (δ_H 3.71) to H-11 (δ_H 1.78) and H-12 (δ_H 0.92) and from H-3 (δ_H 4.15) to methyl groups H-12 (δ_H 0.92) and H-13 (δ_H 0.99), (Figure S2).[18] We also observed that coupling constant between H-3 and H-4 of **1** was 4.0 Hz, while it was only 1.2 Hz in the case of 2*β*,7,3*β*-trihydroxycalamenene 3-*O*-*β*-D-glucoside.[8] Thus, **1** was assigned as a new natural compound, as illustrated in Figure 1, and named abelsaginol (**AS**).

https://doi.org/10.1021/acsomega.2c02974
ACS Omega 2022, 7, 24004−24011

Table 1. Calculated Thermodynamic Parameters (BDEs, PAs, and IEs; kcal mol^{-1}) of AS in the Studied Environments[a]

	BDE				PA				IE			
positions	G	DMSO	P	W	G	DMSO	P	W	G	DMSO	P	W
C1−H	82.4	83.2	82.8	84.5					184.2	116.8	136.3	110.1
C2−H	92.6	92.6	92.5	93.3								
C3−H	96.0	95.7	95.7	96.7								
C4−H	86.9	87.1	86.8	88.1								
C11−H	93.3	93.9	93.5	94.7								
C12−H	99.9	100.4	100.2	101.2								
C14−H	99.9	101.0	100.5	101.8								
C15−H	89.7	90.3	90.2	91.1								
O2−H	106.0	104.7	105.0	107.7								
O3−H	105.0	104.4	104.6	106.8								
O7−H	86.1	84.9	85.0	86.3	339.6	33.4	86.1	48.4				

[a]Abbreviations are as follows: gas, G; pentyl ethanoate, P; dimethyl sulfoxide, DMSO; and water, W.

2.2. The Antioxidant Activity of AS. *2.2.1. The ABTS Antioxidant Assay.* To assess **AS**'s antioxidant activity, the 2,2′-azino-bis(3-ethylbenzothiazoline-6-sulfonic acid (ABTS$^{\bullet+}$) test was used as recommended in the literature,[19,20] with Trolox as a control antioxidant. Under the tested conditions, **AS** was shown to have an ABTS$^{\bullet+}$ scavenging activity two times lower (IC_{50} = 41.04 ± 6.07 mM) than that of Trolox (IC_{50} = 25.16 ± 1.64 mM). To properly evaluate this result, one has to keep in mind that the ABTS experiment is carried out in an organic solvent (dimethyl sulfoxide), hence the data can only show that AS has a lower radical scavenging activity than Trolox in organic solvents. Deprotonation of phenolic groups (i.e., O7−H) in aqueous solutions, on the other hand, can open routes to significantly improve the activity,[21,22] especially at physiological pH. This must be studied further using computational chemistry.

2.2.2. The HOO$^{\bullet}$ Radical Scavenging Activity. 2.2.2.1. Evaluation of the Conformation. The molecular structure suggests that the OH and OMe groups in **AS** can rotate around the single bonds to yield a range of conformers.[23] Thus, after the likely **AS** conformers were screened[24] in the first step, the five lowest-electronic-energy conformers were evaluated utilizing the M06-2*X*/6-311++G(d,p) level of theory (Figure 2). **AS** has the lowest Gibbs free energy value among the conformers, whereas **AS1**−**AS4** have free energies of formation 2.9−5.8 kcal mol^{-1} larger than **AS**. The relative numbers of the conformers were evaluated using the Maxwell−Boltzmann distribution,[25,26] which confirmed that AS was the dominant conformer (>99%); hence, this conformer was investigated further.

2.2.2.2. Thermodynamic Evaluation. Antioxidant activity was assessed using thermodynamic computations that assumed one of the three main radical scavenging pathways,: (i) formal hydrogen transfer (FHT), (ii) single-electron transfer−proton transfer (SETPT), and (iii) sequential proton-loss electron transfer (SPLET).[27] The thermodynamic parameters (ionization energy (IE), bond dissociation enthalpy (BDE), and proton affinity (PA)) of the first step of each pathway for all bonds were calculated for the HOO$^{\bullet}$ antiradical activity of **AS** in pentyl ethanoate as a lipid medium and water at pH 7.4 as an aqueous physiological environment, as well as DMSO to obtain predictions directly comparable to the ABTS assay. The findings are summarized in Table 1.

Tthe lowest BDE(C−H) values were found at C1−H (BDE(C1−H) = 82.4−84.5 kcal mol^{-1}) and C4−H (BDE-(C4−H) = 86.8−88.1 kcal mol^{-1}), whereas those of the O−H bonds were found at O7−H, where BDE(O7−H) = 84.9−86.3 kcal mol^{-1} in all of the studied solvents. By contrast, bond dissociation is not favored at C12(C13)−H or, somewhat unexpectedly, at the O2(O3−-H bonds (BDE = 99.9−107.6 kcal mol^{-1}). These site-specific actions can be explained by the assesment of the spin density distribution, as illustrated in Figure 3. The single electron is stabilized throughout a vast system by resonance, especially in the aromatic ring of the selected radicals. Nonfavored locations, such as C3 or C4, have a spin density distribution centered on the carbon atoms, making product formation difficult.

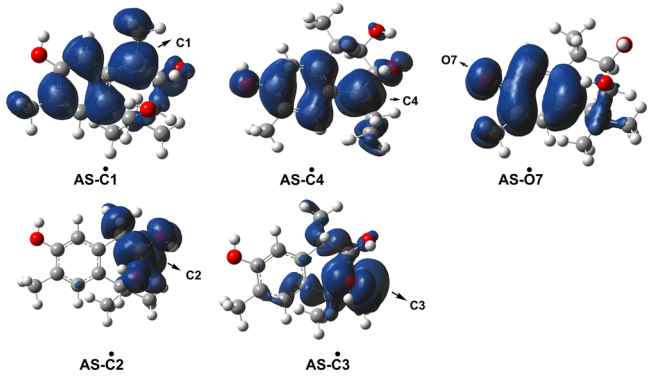

Figure 3. Spin density distribution of the selected radicals

The presence of solvents could slightly affect the BDE values by about 0.8−2.1 kcal mol^{-1}. The BDEs increased in the presence of water but varied in DMSO and the pentyl ethanoate solvents (compared with the gas phase). The IE values were larger than the lowest BDEs in all of the studied solvents (IE = 110.1−184.2 kcal mol^{-1}). This suggests that the single-electron transfer (SET) pathway is not feasible for neutral **AS** in either of the environments. However, the deprotonation at the O7−H bond could preferentially occur in water and DMSO due to the lower PA values compared with the BDE and IE values (PA = 33.4−48.2 kcal mol^{-1}).

Calculations of the Gibbs free energy change ($\Delta G°$, Table 2) in the reaction of **AS** and HOO$^{\bullet}$ indicated that the reaction was only spontaneous in the thermodynamic sense following the hydrogen transfer pathway, particularly at the C1(4)−H and O7−H bonds ($\Delta G°$ = −4.9 to 0.7 kcal mol^{-1}). The FHT reactions at other C−H bonds were not spontaneous, with positive $\Delta G°$ values ($\Delta G°$ = 2.5−20.0 kcal mol^{-1}). At the same

https://doi.org/10.1021/acsomega.2c02974
ACS Omega 2022, 7, 24004−24011

Table 2. Calculated ΔG° (kcal mol^{-1}) of the AS + HOO$^{\bullet}$ Reactions Following the Studied Pathways (FHT, Lose Proton (LP), and SET Mechanisms) in the Studied Media

	FHT				LP				SET			
positions	G	D	P	W	G	D	P	W	G	D	P	W
C1−H	−3.9	−2.8	−3.5	−4.9					160.6	52.1	73.4	29.0
C2−H	5.6	5.8	5.5	3.2								
C3−H	9.1	8.9	8.7	6.5								
C4−H	0.3	0.7	0.2	−1.7								
C11−H	5.7	6.4	5.9	3.9								
C12−H	13.0	13.7	13.3	11.1								
C14−H	13.7	14.9	14.2	12.3								
C15−H	4.3	5.0	4.7	2.5								
O2−H	20.0	18.9	19.1	18.5								
O3−H	19.0	18.5	18.5	17.6								
O7−H	0.0	−0.9	−1.1	−3.0	187.3	83.4	104.2	55.4				

time, the LP and SET reactions were not supported in any of the studied solvents. Thus, in the organic solvents, i.e., pentyl ethanoate and DMSO, and the gas phase, the HOO$^{\bullet}$ radical scavenging activity is defined by the FHT pathway, whereas deprotonation and stable states of **AS** should be considered in polar environments such as water at pH 7.40.

2.2.2.3. Kinetic Study. To examine the feasibility and kinetics of electron transfer reactions from the deprotonated species, the protonation state of **AS** at physiological pH must be determined. Protonation at the O7−H location is possible with the **AS** structure. The pK_a values of **AS** were calculated according to the literature,[28,29] and the results are shown in Figure 4.

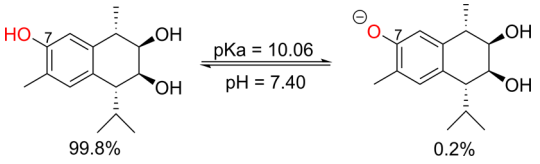

Figure 4. Acid dissociation equilibrium of **AS** at pH 7.40.

The pK_a value calculated for the O7−H group was 10.06. Thus, in a pH 7.4 aqueous solution, there is still a non-negligible amount of the monoanionic state (O7H, 0.2% (Figure 4). The kinetic evaluation of the HOO$^{\bullet}$ antiradical activity of **AS** occurred in water at pH 7.4; therefore, has to take into account both the neutral and anionic species.

The kinetic calculations in the gas phase (Table S3 and Figure 5) showed that the H-abstraction of the O7−H bond defines the FHT reaction ($k_{(O7-H)}$ = 1.26 × 10^3 M^{-1} s^{-1}, Γ = 99.4%). FHT reactions of the C1(C4)−H bonds played a minor role (Γ = 0.6%). Thus, the rate constants of the FHT reactions in the solvents, i.e. DMSO, pentyl ethanoate, and water, were computed on the basis of the H-abstraction of the hydroxyl group. Therefore, the total rate constant ($k_{overall}$) of **AS**'s antiradical activity against the HOO$^{\bullet}$ radical in the aqueous physiological environment can be calculated using eqs 1 and 2. Table 3 and Figure 5 show the final results.

In the organic solvents:

$$k_{overall} = k_{app}(O7 - H) \quad (1)$$

In the aqueous solution:

$$k_{overall} = k_f(SET - anion) + k_f(O7 - H\ (neutral)) \quad (2)$$

As shown in Table 3, **AS** exhibited a low HOO$^{\bullet}$ radical scavenging activity in the organic solvents (pentyl ethanoate and DMSO) with k_{app} = 5.90 × 10^2 and 1.50 × 10^2 M^{-1} s^{-1}, respectively. In the lipid medium, the HOO$^{\bullet}$ trapping capability of **AS** was lower than those of typical antioxidants such as Trolox ($k_{overall}$ = 3.40 × 10^3 M^{-1} s^{-1}),[30] BHT ($k_{overall}$ = 1.70 × 10^4 M^{-1} s^{-1}),[31] resveratrol ($k_{overall}$ = 1.31 × 10^4 M^{-1} s^{-1}),[32] and ascorbic acid ($k_{overall}$ = 5.71 × 10^3 M^{-1} s^{-1}).[33] This activity was also lower than that of samwirin A ($k_{overall}$ = 6.70 × 10^3 M^{-1} s^{-1}).[20] However, **AS** exhibited significant hydroperoxyl antiradical activity ($k_{overall}$ = 9.00 × 10^6 M^{-1} s^{-1}) in water at pH 7.40. The activity follows the SET reaction pathway of the anion state (Γ = 100%). The FHT reaction of the O7−H bond had no contribution to the overall rate constant. **AS** exhibited a higher HOO$^{\bullet}$ radical scavenging activity than Trolox (k = 8.96 × 10^4 M^{-1} s^{-1})[30] and BHT ($k_{overall}$ = 2.51 × 10^5 M^{-1} s^{-1})[31] but a slightly lower activity than resveratrol (k = 5.62 × 10^7 M^{-1} s^{-1})[32] and ascorbic acid (k = 9.97 × 10^7 M^{-1} s^{-1}).[33] Based on the computed data, **AS** is a promising radical scavenger in the aqueous physiological environment.

*2.2.3. The Antiradical Activity of **AS** in an Aqueous Solution against Conventional Free Radicals.* Due to its mild reactivity, the HOO$^{\bullet}$ radical is regarded a model free radical for evaluating the antiradical activities of organic compounds.[33,34] Studies on the radical scavenging ability of natural products against other common reactive oxygen and nitrogen species, such as HO$^{\bullet}$, $CH_3O^{\bullet}$, $CCl_3O^{\bullet}$, HOO$^{\bullet}$, $CH_3OO^{\bullet}$, $CCl_3OO^{\bullet}$, NO, NO_2, $O_2^{\bullet-}$, $SO_4^{\bullet-}$ and $N_3^{\bullet}$, are critical to provide useful information regarding their antioxidant activities.[35,36] Therefore, next the antiradical activity of **AS** was also modeled against these free radicals following the main mechanism (the SET reaction) in water at pH 7.40. The results are shown in Table 4

It was found that **AS** should have moderate activity against $CH_3O^{\bullet}$, $CH_3OO^{\bullet}$, $CCl_3OO^{\bullet}$, NO_2, and $SO_4^{\bullet-}$ radicals, with k_f values ranging from 4.00 × 10^3 to 1.52 × 10^7 M^{-1} s^{-1}, whereas HO$^{\bullet}$, $CCl_3O^{\bullet}$, NO, $O_2^{\bullet-}$, and $N_3^{\bullet}$ radicals could not be removed by **AS** under the examined conditions. Compared with fraxin[35] and usnic acid,[36] **AS** exhibited lower HO$^{\bullet}$, $CCl_3O^{\bullet}$, and $N_3^{\cdot}$ antiradical activity following the SET reaction but was more active against peroxyl radicals, i.e. HOO$^{\bullet}$ and $CH_3OO^{\bullet}$.

https://doi.org/10.1021/acsomega.2c02974
ACS Omega 2022, 7, 24004−24011

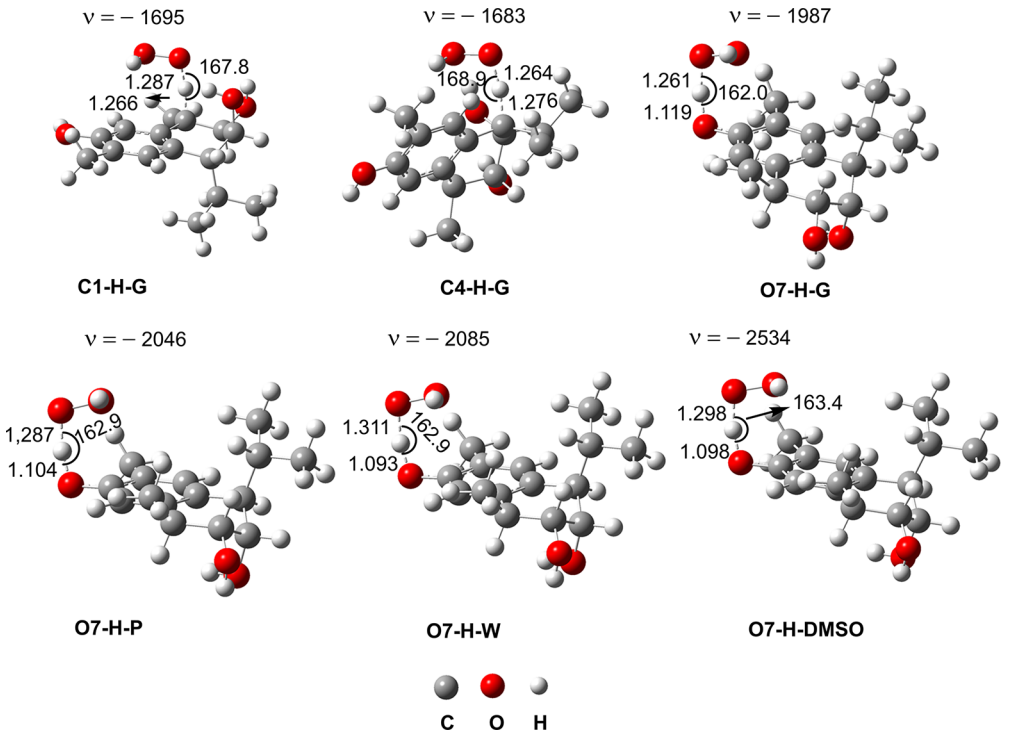

Figure 5. Optimized transition state (TS) structures and their imaginary frequencies (ν, cm^{-1}) according to the FHT reaction of the **AS** + $HOO^{\bullet}$ reaction (ν, cm^{-1}. Abbreviations are as follows: dimethyl sulfoxide, DMSO; P, pentyl ethanoate; G, gas phase; and W, water).

Table 3. Calculated $\Delta G^{\neq}$ (kcal mol^{-1}), Tunneling Corrections (κ), Molar Fractions (f), Rate Constants (k_{app}, k_f, and $k_{overall}$; M^{-1} s^{-1}), and Branching Ratios (Γ, %) in the AS + $HOO^{\bullet}$ Reaction[a]

solvents	mechanisms	$\Delta G^{\neq}$	k	k_{app}	f	k_f	Γ
P	FHT	16.6	145.5	5.90×10^2			100.0
DMSO	FHT	17.6	183.4	1.50×10^2			100.0
W	SET	3.8	16.4[b]	4.50×10^9	0.002	9.00×10^6	100.0
	FHT	16.7	605.3	2.20×10^3	0.998	2.20×10^3	0.0
	$k_{overall}$					9.00×10^6	

[a]At 298.15 K in P, DMSO, and W solvents. [b]The nuclear reorganization energy (λ, kcal mol^{-1}); $k_f = f \cdot k_{app}$ and $\Gamma = k_f \cdot 100/k_{overall}$

Table 4. Calculated $\Delta G^{\neq}$, λ, (kcal mol^{-1}), Diffusion-Limited Rate Constant (k_D), k_{app}, and k_f (M^{-1} s^{-1}) of the Reaction Between AS^- and Chosen Radicals in Aqueous Solution at pH 7.4[a]

radicals	$\Delta G^{\neq}$	λ	k_D	k_{app}	k_f[b]
$HO^{\bullet}$	18.7	4.4	8.50×10^9	1.20×10^{-1}	2.40×10^{-4}
$CH_3O^{\bullet}$	0.0	5.6	8.10×10^9	8.10×10^9	1.62×10^7
$CCl_3O^{\bullet}$	17.5	22.2	7.60×10^9	9.30×10^{-1}	1.86×10^{-3}
$HOO^{\bullet}$	3.8	16.4	8.20×10^9	4.50×10^9	9.00×10^6
$CH_3OO^{\bullet}$	4.6	15.8	8.00×10^9	2.00×10^9	4.00×10^6
$CCl_3OO^{\bullet}$	0.2	17.9	7.60×10^9	7.60×10^9	1.52×10^7
NO	79.4	15.3	8.30×10^9	3.90×10^{-46}	7.80×10^{-49}
NO_2	0.5	28.8	8.10×10^9	8.10×10^9	1.62×10^7
$O_2^{\bullet-}$	43.0	18.2	7.20×10^9	1.80×10^{-19}	3.60×10^{-22}
$SO_4^{\bullet-}$	8.90	18.6	7.90×10^9	2.00×10^6	4.00×10^3
$N_3^{\bullet}$	20.3	3.5	7.00×10^9	8.10×10^{-3}	1.62×10^{-5}

[a]According to the SET reaction. [b]$k_f = f \cdot k_{app}$ and $f(AS^-) = 0.002$.

3. CONCLUSION

The novel sesquiterpenoid compound **AS** was successfully isolated and identified from *A. sagittifolius*. **AS** showed a low $HOO^{\bullet}$ radical scavenging activity in the DMSO solvent ($k_{overall}$ = 1.50×10^2 M^{-1} s^{-1}) both in silico and in the experimental $ABTS^{\bullet+}$ test. Similar results were also found for its activity in the lipid medium, i.e., the pentyl ethanoate solvent. Thus, **AS** is predicted to be a weak radical scavenger in lipid media. However, **AS** exhibited good $HOO^{\bullet}$ antiradical activity in water at pH 7.40 ($k_{overall}$ = 9.00×10^6 M^{-1} s^{-1}), primarily via the SET reaction of the anion state. **AS** is predicted to exhibit moderate activity against $CH_3O^{\bullet}$, $CH_3OO^{\bullet}$, $CCl_3OO^{\bullet}$, NO_2, and $SO_4^{\bullet-}$ radicals, with k_f = 4.00×10^3 − 1.52×10^7 M^{-1} s^{-1},

https://doi.org/10.1021/acsomega.2c02974
ACS Omega 2022, 7, 24004−24011

whereas it is expected to exhibit weak activity against $HO^{\bullet}$, $CCl_3O^{\bullet}$, NO, $O_2^{\bullet-}$, and $N_3^{\bullet}$ radicals. Compared with natural typical antioxidants, the activity of **AS** in water at pH 7.40 is generally higher than those of Trolox and BHT. Thus, **AS** is a promising natural antioxidant in the aqueous physiological environment.

4. EXPERIMENTAL AND COMPUTATIONAL METHODS

4.1. Experimental Section. *4.1.1. Plant Materials.* The plant samples of *A. sagittifolius* were collected from Bao mountain (20°01′04.0″N 105°41′04.9″E), Vinh Loc district, Thanh Hóa province, Vietnam, in October 2020, which was the harvest season for *A. sagittifolius* growing in this area. The plant was identified by Prof. Dr. Tran The Bach of the Institute of Ecology and Biological Resources, Vietnam Academy of Science and Technology. The plant specimens (SB-2020) were deposited at the Botanical Museum (HN) Institute of Ecology and Biological Resources, 18 Hoang Quoc Viet, Cau Giay, Hanoi, Vietnam.

4.1.2. General Experimental Procedures. Solvents and chemicals used for extraction and isolation met experimental standards. Column chromatography was performed on 40−63 μm silica gel (Merck) and reverse-phase silica gel RP-18 (YMC). Thin layer chromatography (TLC) was performed on precoated plates (Merck 60 F_{254}), which were visualized using a 254 nm ultraviolet lamp or a 10% sulfuric acid solution spray. Nuclear magnetic resonance (NMR) spectra were recorded on a 500 MHz Bruker Avance instrument. The HR-ESI-MS spectra were obtained using an Agilent 6530 Accurate Mass Q-TOF LC/MS system. The ABTS (2,2′-azino-di(3-ethyl-benzthiazoline sulfonic acid) assay was performed following the literature procedure.[19,20]

4.2. Computational Details. All DFT calculations were carried out with the Gaussian 09 suite of programs.[37] The M06-2X functional,[38] one of the most dependable tools for studying the thermodynamics and kinetics of radical processes,[21,30,33,38−41] and the 6-311++G(d,p) basis set were used for all calculations. The kinetics calculations were carried out using the quantum mechanics-based test for overall free radical scavenging activity (QM-ORSA) protocol,[33] with the SMD solvation model[42] for water, DMSO, and pentyl ethanoate solvents.[21,41,43−48]

Using the transition state theory (TST) at 298.15 K and 1 M standard state, the rate constant (k) was computed as follows:[43−47]

$$k = \sigma\kappa\frac{k_B T}{h}e^{-(\Delta G^{\neq})/RT} \quad (3)$$

where σ is the reaction symmetry number,[49,50] $\Delta G‡$ is the Gibbs free energy of activation, κ contains the tunneling corrections calculated using the Eckart barrier,[51] h is the Planck constant, and k_B is the Boltzmann constant.

The reaction barriers of SET reactions in media were determined using the Marcus theory.[52,53] The equations used to calculate the Gibbs free energy change of reaction ($\Delta G‡$) for the SET pathway are

$$\Delta G_{SET}^{\neq} = \frac{\lambda}{4}\left(1 + \frac{\Delta G_{SET}^{0}}{\lambda}\right)^2 \quad (4)$$

$$\lambda \approx \Delta E_{SET} - \Delta G_{SET}^{0} \quad (5)$$

where ΔG^0_{SET} is the standard Gibbs free energy change of the reaction, while ΔE_{SET} is the nonadiabatic energy difference between reactants and vertical products for SET.[54,55] A correction was applied to rate constants that were close to the diffusion limit.[33] The apparent rate constants (k_{app}) for an irreversible bimolecular diffusion-controlled reaction were computed using the Collins−Kimball theory in solvents at 298.15 K;[56] the steady-state Smoluchowski rate constant (k_D) was estimated as follows using the literature:[33,57]

$$k_{app} = \frac{k_{TST}k_D}{k_{TST} + k_D} \quad (6)$$

$$k_D = 4\pi R_{AB} D_{AB} N_A \quad (7)$$

$D_{AB} = D_A + D_B$ (D_{AB} is the mutual diffusion coefficient of the reactants A and B),[56,58] where D_A or D_B is determined using the Stokes−Einstein formulation (8).[59,60]

$$D_{A/B} = \frac{k_B T}{6\pi a_{A/B}} \quad (8)$$

Here η is the viscosity of the solvents (i.e., η(pentyl ethanoate) = 8.62×10^{-4} Pa s and $\eta(H_2O) = 8.91 \times 10^{-4}$ Pa s) and a is the radius of the solute.

To avoid overpenalizing entropy losses in solution, the solvent cage effects were added using Okuno's adjustments,[61] which were modified with the free-volume theory according to the Benson correction.[33,62−64]

For species with numerous conformers, all of them were energy minimized,[23] and the lowest-electronic-energy conformer was included in the study. The existence of only a single imaginary frequency was the defining feature of all transition stages. To verify that each transition state was accurately related to the precomplex and postcomplex, intrinsic coordinate calculations (IRCs) were performed.

■ ASSOCIATED CONTENT

Supporting Information

The Supporting Information is available free of charge at https://pubs.acs.org/doi/10.1021/acsomega.2c02974.

NMR spectra, thermodynamic parameters, Cartesian coordinates, and frequencies and energies of all of the transition states in the studied environments (PDF)

■ AUTHOR INFORMATION

Corresponding Authors

Thuc Dinh Ngoc − *Department of Science and Technology Management, Hong Duc University, Thanh Hóa, Thanh Hóa 40000, Vietnam;* orcid.org/0000-0001-6307-5139; Email: dinhngocthuc@hdu.edu.vn

Quan V. Vo − *The University of Danang − University of Technology and Education, Danang 550000, Vietnam;* orcid.org/0000-0001-7189-9584; Email: vvquan@ute.udn.vn

Authors

Mai Vu Thi Ha − *Department of Science and Technology Management, Hong Duc University, Thanh Hóa, Thanh Hóa 40000, Vietnam*

Thanh Nguyen Le − *Institute of Marine Biochemistry (IMBC), Graduate University of Science and Technology (GUST), Vietnam Academy of Science and Technology (VAST), Hanoi 10000, Vietnam*

https://doi.org/10.1021/acsomega.2c02974
ACS Omega 2022, 7, 24004−24011

Hue Vu Thi − *Institute of Marine Biochemistry (IMBC), Graduate University of Science and Technology (GUST), Vietnam Academy of Science and Technology (VAST), Hanoi 10000, Vietnam*

Thi Van Anh Nguyen − *University of Science and Technology of Hanoi (USTH), Vietnam Academy of Science and Technology (VAST), Hanoi 10000, Vietnam*

Adam Mechler − *Department of Biochemistry and Chemistry, La Trobe University, Melbourne, Victoria 3086, Australia;* orcid.org/0000-0002-6428-6760

Nguyen Thi Hoa − *The University of Danang − University of Technology and Education, Danang 550000, Vietnam*

Complete contact information is available at: https://pubs.acs.org/10.1021/acsomega.2c02974

Notes

The authors declare no competing financial interest.

REFERENCES

(1) Coombes, A. J. *The A to Z of Plant Names: A Quick Reference Guide to 4000 Garden Plants*; Timber Press: Portland, OR, 2012.

(2) *Abelmoschus sagittifolius* (Kurz) Merr. *Plants of the World Online*. Royal Botanical Gardens, Kew: Richmond, England. http://powo.science.kew.org/taxon/urn:lsid:ipni.org:names:558042-1 (accessed on 2021-09-02).

(3) Patil, P.; Sutar, S.; Malik, S. K.; John, J.; Yadav, S.; Bhat, K. V. Numerical taxonomy of Abelmoschus Medik.(Malvaceae) in India. *Bangladesh J. Plant Taxon.* **2015**, *22* (2), 87−98.

(4) Pham, T.; Thi, Q. N.; Cam, L. N.; Minh, D. T.; Van, G. T. The effects of plant growth regulators on in-vitro culture of abelmoschus sagittifolius. *Plant Cell Biotechnol. Mol. Biol.* **2021**, 32−40.

(5) Pham, T. H.; Nguyen, Q. N.; Pham, T. N.; Lai, V. H.; Phan, V. T.; Nguyen, V. H.; Dang, M. T.; Nguyen, T. H. L.; Duong, T. P. T.; Pham, T. H. N. Study on Morphological and Microscopic Characteristics of Abelmoschus sagittifolius (Kurz) Merr. in Vietnam. *VNU J. Sci. Med. Pharm. Sci.* **2021**, *37* (2), 24−31.

(6) State Administration of Traditional Chines Medicine "Chinese Materia Medica" Editorial Bord. *Zhonghua ben cao*, Vol. *15*; Shanghai Scientific and Technology Press: Shanghai, 1999; p 643.

(7) Bich, D.; Chung, D.; Chuong, B.; Dong, N.; Dam, D. T.; Hien, P.; Lo, V.; Mai, P.; Man, P.; Nhu, D. *The Medicinal Plants and Animals in Vietnam*; Science and Technology Publishing House: Hanoi, Vietnam, **2004**.

(8) Li, J.; Ye, G.-y.; Liu, H.-l.; Wang, Z.-h. Complete chloroplast genomes of three important species, Abelmoschus moschatus, A. manihot and A. sagittifolius: Genome structures, mutational hotspots, comparative and phylogenetic analysis in Malvaceae. *PloS one* **2020**, *15* (11), No. e0242591.

(9) Chen, D.-L.; Li, G.; Liu, Y.-Y.; Ma, G.-X.; Zheng, W.; Sun, X.-B.; Xu, X.-D. A new cadinane sesquiterpenoid glucoside with cytotoxicity from Abelmoschus sagittifolius. *Nat. Prod. Res.* **2019**, *33* (12), 1699−1704.

(10) Chen, D.-L.; Zhang, X.-P.; Ma, G.-X.; Wu, H.-F.; Yang, J.-S.; Xu, X.-D. A new sesquiterpenoid quinone with cytotoxicity from Abelmoschus sagittifolius. *Nat. Prod. Res.* **2016**, *30* (5), 565−569.

(11) Thuc, D. N.; Huong, V. T.; Mai, V. T. H.; Thanh, L. N. Terpenoid Compounds from the Roots of Abelmoschus sagittifolius (Kurz) Merr. *J. Med. Pharm.* **2021**, *17*, 16−20.

(12) Loscalzo, J. Oxidant stress: a key determinant of athero-thrombosis. *Biochem. Soc. Trans.* **2003**, *31* (5), 1059−1061.

(13) Ferroni, P.; Santilli, F.; Cavaliere, F.; Simeone, P.; Costarelli, L.; Liani, R.; Tripaldi, R.; Riondino, S.; Roselli, M.; Davi, G.; et al. Oxidant stress as a major determinant of platelet activation in invasive breast cancer. *Int. J. Cancer* **2017**, *140* (3), 696−704.

(14) Moore, J. D.; Harned, A. M.; Henle, J.; Flynn, D. L.; Hanson, P. R. Scavenge− ROMP− Filter: A Facile Strategy for Soluble Scavenging via Norbornenyl Tagging of Electrophilic Reagents. *Org. Lett.* **2002**, *4* (11), 1847−1849.

(15) Tulipani, S.; Mezzetti, B.; Capocasa, F.; Bompadre, S.; Beekwilder, J.; De Vos, C. R.; Capanoglu, E.; Bovy, A.; Battino, M. Antioxidants, phenolic compounds, and nutritional quality of different strawberry genotypes. *J. Agric. Food Chem.* **2008**, *56* (3), 696−704.

(16) Apak, R. a.; Özyürek, M.; Güçlü, K.; Çapanoğlu, E. Antioxidant activity/capacity measurement. 1. Classification, physicochemical principles, mechanisms, and electron transfer (ET)-based assays. *J. Agric. Food Chem.* **2016**, *64* (5), 997−1027.

(17) Ozkan, G.; Franco, P.; De Marco, I.; Xiao, J.; Capanoglu, E. A review of microencapsulation methods for food antioxidants: Principles, advantages, drawbacks and applications. *Food Chem.* **2019**, *272*, 494−506.

(18) Boonsri, S.; Karalai, C.; Ponglimanont, C.; Chantrapromma, S.; Kanjana-Opas, A. Cytotoxic and antibacterial sesquiterpenes from Thespesia populnea. *J. Nat. Prod.* **2008**, *71* (7), 1173−1177.

(19) Re, R.; Pellegrini, N.; Proteggente, A.; Pannala, A.; Yang, M.; Rice-Evans, C. Antioxidant activity applying an improved ABTS radical cation decolorization assay. *Free Radic. Biol. Med.* **1999**, *26* (9−10), 1231−1237.

(20) Dinh Ngoc, T.; Ha, M. V. T.; Nguyen Le, T.; Nguyen, T. V. A.; Mechler, A.; Hoa, N. T.; Vo, Q. V. Antioxidant Activity of Natural Samwirin A: Theoretical and Experimental Insights. *ACS omega* **2021**, *6* (41), 27546−27551.

(21) Vo, Q. V.; Bay, M. V.; Nam, P. C.; Quang, D. T.; Flavel, M.; Hoa, N. T.; Mechler, A. Theoretical and Experimental Studies of the Antioxidant and Antinitrosant Activity of Syringic Acid. *J. Org. Chem.* **2020**, *85* (23), 15514−15520.

(22) Vo, Q. V.; Thong, N. M.; Le Huyen, T.; Nam, P. C.; Tam, N. M.; Hoa, N. T.; Mechler, A. A thermodynamic and kinetic study of the antioxidant activity of natural hydroanthraquinones. *RSC Adv.* **2020**, *10* (34), 20089−20097.

(23) Dzib, E.; Merino, G. The hindered rotor theory: A review. *WIREs Comput. Mol. Sci.* **2022**, *12*, No. e1583.

(24) Hehre, W.; Yu, J.; Klunzinger, P.; Lou, L. *Spartan Software.*; Wavefunction. Inc.: Irvine, CA, 2000.

(25) Galano, A.; Alvarez-Idaboy, J. R. Glutathione: mechanism and kinetics of its non-enzymatic defense action against free radicals. *RSC Adv.* **2011**, *1* (9), 1763−1771.

(26) Vo, Q. V.; Tam, N. M.; Bay, M. V.; Mechler, A. The radical scavenging activity of natural ramalin: A mechanistic and kinetic study. *Chem. Phys. Lett.* **2020**, *739*, 137004.

(27) Ingold, K. U.; Pratt, D. A. Advances in radical-trapping antioxidant chemistry in the 21st century: a kinetics and mechanisms perspective. *Chem. Rev.* **2014**, *114* (18), 9022−9046.

(28) Galano, A.; Pérez-González, A.; Castañeda-Arriaga, R.; Muñoz-Rugeles, L.; Mendoza-Sarmiento, G.; Romero-Silva, A.; Ibarra-Escutia, A.; Rebollar-Zepeda, A. M.; León-Carmona, J. R.; Hernández-Olivares, M. A.; Alvarez-Idaboy, J. R. Empirically Fitted Parameters for Calculating p K a Values with Small Deviations from Experiments Using a Simple Computational Strategy. *J. Chem. Inf. Model.* **2016**, *56* (9), 1714−1724.

(29) Vo, Q. V.; Hoa, N. T.; Nam, P. C.; Quang, D. T.; Mechler, A. In Silico Evaluation of the Radical Scavenging Mechanism of Mactanamide. *ACS Omega* **2020**, *5* (37), 24106−24110.

(30) Alberto, M. E.; Russo, N.; Grand, A.; Galano, A. A physicochemical examination of the free radical scavenging activity of Trolox: mechanism, kinetics and influence of the environment. *Phys. Chem. Chem. Phys.* **2013**, *15* (13), 4642−4650.

(31) Boulebd, H. Radical scavenging behavior of butylated hydroxytoluene against oxygenated free radicals in physiological environments: Insights from DFT calculations. *Int. J. Chem. Kinet.* **2022**, *54*, 50−57.

(32) Iuga, C.; Alvarez-Idaboy, J. R. l.; Russo, N. Antioxidant activity of trans-resveratrol toward hydroxyl and hydroperoxyl radicals: a quantum chemical and computational kinetics study. *J. Org. Chem.* **2012**, *77* (8), 3868−3877.

(33) Galano, A.; Alvarez-Idaboy, J. R. A computational methodology for accurate predictions of rate constants in solution: Application to the assessment of primary antioxidant activity. *J. Comput. Chem.* **2013**, *34* (28), 2430−2445.
(34) Galano, A.; Raúl Alvarez-Idaboy, J. Computational strategies for predicting free radical scavengers' protection against oxidative stress: Where are we and what might follow? *Int. J. Quantum Chem.* **2019**, *119* (2), No. e25665.
(35) Nam, P. C.; Thong, N. M.; Hoa, N. T.; Quang, D. T.; Hoang, L. P.; Mechler, A.; Vo, Q. V. Is natural fraxin an overlooked radical scavenger? *RSC Adv.* **2021**, *11* (24), 14269−14275.
(36) Hoa, N. T.; Van Bay, M.; Mechler, A.; Vo, Q. V. Is usnic acid a promising radical scavenger? *ACS omega* **2020**, *5* (28), 17715−17720.
(37) Frisch, M. J.; Trucks, G. W.; Schlegel, H. B.; Scuseria, G. E.; Robb, M. A.; Cheeseman, J. R.; Scalmani, G.; Barone, V.; Mennucci, B.; Petersson, G. A. et al. *Gaussian 09*; Gaussian, Inc.: Wallingford, CT, 2009.
(38) Zhao, Y.; Truhlar, D. G. How Well Can New-Generation Density Functionals Describe the Energetics of Bond-Dissociation Reactions Producing Radicals? *J. Phys. Chem. A* **2008**, *112* (6), 1095−1099.
(39) Galano, A.; Alvarez-Idaboy, J. R. Kinetics of radical-molecule reactions in aqueous solution: A benchmark study of the performance of density functional methods. *J. Comput. Chem.* **2014**, *35* (28), 2019−2026.
(40) Alvarez-Idaboy, J. R. l.; Galano, A. On the Chemical Repair of DNA Radicals by Glutathione: Hydrogen Vs Electron Transfer. *J. Phys. Chem. B* **2012**, *116* (31), 9316−9325.
(41) Dzib, E.; Cabellos, J. L.; Ortíz-Chi, F.; Pan, S.; Galano, A.; Merino, G. Eyringpy: A Program for Computing Rate Constants in the Gas Phase and in Solution. *Int. J. Quantum Chem.* **2019**, *119* (2), No. e25686.
(42) Marenich, A. V.; Cramer, C. J.; Truhlar, D. G. Universal Solvation Model Based on Solute Electron Density and on a Continuum Model of the Solvent Defined by the Bulk Dielectric Constant and Atomic Surface Tensions. *J. Phys. Chem. B* **2009**, *113* (18), 6378−6396.
(43) Evans, M. G.; Polanyi, M. Some applications of the transition state method to the calculation of reaction velocities, especially in solution. *Trans. Faraday Soc.* **1935**, *31*, 875−894.
(44) Eyring, H. The Activated Complex in Chemical Reactions. *J. Chem. Phys.* **1935**, *3* (2), 107−115.
(45) Truhlar, D. G.; Hase, W. L.; Hynes, J. T. Current Status of Transition-State Theory. *J. Phys. Chem.* **1983**, *87* (15), 2664−2682.
(46) Furuncuoglu, T.; Ugur, I.; Degirmenci, I.; Aviyente, V. Role of chain transfer agents in free radical polymerization kinetics. *Macromolecules* **2010**, *43* (4), 1823−1835.
(47) Vélez, E.; Quijano, J.; Notario, R.; Pabón, E.; Murillo, J.; Leal, J.; Zapata, E.; Alarcón, G. A computational study of stereospecifity in the thermal elimination reaction of menthyl benzoate in the gas phase. *J. Phys. Org. Chem.* **2009**, *22* (10), 971−977.
(48) Dzib, E.; Cabellos, J. L.; Ortiz-Chi, F.; Pan, S.; Galano, A.; Merino, G. Eyringpy: A program for computing rate constants in the gas phase and in solution. *Int. J. Quantum Chem.* **2019**, *119*, No. e25686.
(49) Pollak, E.; Pechukas, P. Symmetry numbers, not statistical factors, should be used in absolute rate theory and in Broensted relations. *J. Am. Chem. Soc.* **1978**, *100* (10), 2984−2991.
(50) Fernández-Ramos, A.; Ellingson, B. A.; Meana-Pañeda, R.; Marques, J. M.; Truhlar, D. G. Symmetry numbers and chemical reaction rates. *Theor. Chem. Acc.* **2007**, *118* (4), 813−826.
(51) Eckart, C. The penetration of a potential barrier by electrons. *Phys. Rev.* **1930**, *35* (11), 1303.
(52) Marcus, R. A. Chemical and Electrochemical Electron-Transfer Theory. *Annu. Rev. Phys. Chem.* **1964**, *15* (1), 155−196.
(53) Marcus, R. A. Electron Transfer Reactions in Chemistry. *Theory and Experiment. Rev. Mod. Phys.* **1993**, *65* (3), 599.
(54) Nelsen, S. F.; Blackstock, S. C.; Kim, Y. Estimation of inner shell Marcus terms for amino nitrogen compounds by molecular orbital calculations. *J. Am. Chem. Soc.* **1987**, *109* (3), 677−682.
(55) Nelsen, S. F.; Weaver, M. N.; Luo, Y.; Pladziewicz, J. R.; Ausman, L. K.; Jentzsch, T. L.; O'Konek, J. J. Estimation of electronic coupling for intermolecular electron transfer from cross-reaction data. *J. Phys. Chem. A* **2006**, *110* (41), 11665−11676.
(56) Collins, F. C.; Kimball, G. E. Diffusion-Controlled Reaction Rates. *J. Colloid Sci.* **1949**, *4* (4), 425−437.
(57) Von Smoluchowski, M. Mathematical Theory of the Kinetics of the Coagulation of Colloidal Solutions. *Z. Phys. Chem.* **1917**, *92*, 129.
(58) Truhlar, D. G. Nearly encounter-controlled reactions: The equivalence of the steady-state and diffusional viewpoints. *J. Chem. Educ.* **1985**, *62* (2), 104.
(59) Einstein, A. Über die von der molekularkinetischen Theorie der Wärme geforderte Bewegung von in ruhenden Flüssigkeiten suspendierten Teilchen. *Ann. Phys.* **1905**, *322*, 549−560.
(60) Stokes, G. G. *Mathematical and Physical Papers*. University Press: Cambridge, U.K., 2009.
(61) Okuno, Y. Theoretical Investigation of the Mechanism of the Baeyer-Villiger Reaction in Nonpolar Solvents. *Chem.: Eur. J.* **1997**, *3* (2), 212−218.
(62) Benson, S. *The foundations of chemical kinetics*. R.E. Krieger: Malabar, FL, 1982.
(63) Iuga, C.; Alvarez-Idaboy, J. R.; Vivier-Bunge, A. ROS Initiated Oxidation of Dopamine under Oxidative Stress Conditions in Aqueous and Lipidic Environments. *J. Phys. Chem. B* **2011**, *115* (42), 12234−12246.
(64) Alvarez-Idaboy, J. R.; Reyes, L.; Mora-Diez, N. The mechanism of the Baeyer−Villiger rearrangement: quantum chemistry and TST study supported by experimental kinetic data. *Org. Biomol. Chem.* **2007**, *5* (22), 3682−3689.

https://doi.org/10.1021/acsomega.2c02974
ACS Omega 2022, 7, 24004−24011